DOI: 10.1002/app.51710

Dynamic electrical and mechanical properties of epoxy/silver nanowires composites

Vincent Bedel[1,2] | **Antoine Lonjon**[1] | **Éric Dantras**[1] | **Michel Bouquet**[2] | **Colette Lacabanne**[1]

[1]CIRIMAT, Physique des Polymères, Université de Toulouse, Toulouse, France

[2]Institut de Recherche Technologique (IRT) Saint Exupéry, Toulouse, France

Correspondence
Antoine Lonjon, CIRIMAT, Physique des Polymères, Université de Toulouse, 118 route de Narbonne 31062, Toulouse Cedex 09, France.
Email: antoine.lonjon@univ-tlse3.fr

Funding information
Agence Nationale de la Recherche; Commissariat Général aux Investissements

Abstract

The aim of this work is to study electrically conductive composites from an epoxy matrix loaded with silver nanowires (AgNWs). Dynamic mechanical analysis (DMA) and dynamic dielectric spectroscopy (DDS) were used to study the molecular mobility of the epoxy matrix and its epoxy/AgNWs composites. The influence of the epoxy/amine ratio on the macroscopic properties was analyzed. The loss modulus of the epoxy matrix highlights two major relaxations, β and α. The β relaxation is due to the localized mobility initiated by hydroxyl groups. The α trelaxation is the anelastic effect liberated at the glass transition. The introduction of a small amount of AgNWs (<8 vol%) has practically no influence on the mechanical properties of the glassy state. For the rubbery state, AgNWs cause an increase in the storage modulus as a function of the filler content. The loss modulus profile is modified: The ω relaxation due to heterogeneities of the 3D network is observed independently from the hydration level of composites. The magnitude of the α mode is increased due to the stick–slip phenomenon. Moreover, it is shifted toward lower temperatures upon the introduction of AgNWs. In other words, the activation enthalpy decreases for both modes. Electrical study through DDS and conductivity measurement of epoxy/AgNWs composites shows the consequence of a lower relative degree of conversion caused by the insertion of AgNWs. Epoxy/AgNWs composites allow us to obtain one of the highest values of the electrical conductivity for polymer-based composites without any drastic evolution of mechanical properties.

KEYWORDS

coating, dynamic mechanical analysis, epoxy nanocomposite, silver nanowires dynamic dielectric spectroscopy, Thermal properties

1 | INTRODUCTION

The use of thermoset matrices reinforced by carbon fibers (CFRP) is in steady increase in aeronautic since the last decades, mainly for the structural parts.[1] It permits to obtain a weight reduction; however, their electrical conductivity is widely lower than aluminum.[2] The consequences could be some structural damages under lightning strike. The use of metallic part in surface is the current solution for the lightning strike protections (LSP): metallic foil, perforated metallic foil, metallic mesh, or expended metal foil applied on the top of structural plies.[3,4] The LSP design depends on the area to be protected.[5] All of these solutions are efficient but they cause a slight overweight and they are complex to process due to their rigidity.

Conductive polymer composites filled with conductive metallic fillers could be an alternative due to the high electrical conductivity of metal which are a thousand time more conductive than the carbon ones.[6] Riviere et al.[7] have obtained an electrical conductive level slightly higher than 10^2 S.m^{-1} with a polymer composite filled with 20% in volume of silver particles. This high level of electrical conduction is obtained at the expense of the mechanical properties and the weight. Several kinds of metallic fillers have been testing, and the highest level of conductivity reached 10^2 S.m^{-1} for a homogenous dispersion.[8–14] The recent works on conductive polymer composites filled with high aspect ratio metallic fillers allows obtaining a percolation threshold for a small volume fraction (<1%) and keep mechanical properties.[15–20]

The aim of this work is to study the mechanical and dielectric behaviors of conductive composites epoxy/silver nanowires (AgNWs). This composite is designed to develop a high conductive coating with low filler content[21] (≤8% in volume) and could be used as an LSP of aircrafts.

First, the influence of the resin/hardener ratio is studied by mechanical and dielectric relaxation spectroscopies. A similar study is carried out to highlight the effect of the moisture on the matrix. Finally, the investigation of AgNWs influence on mechanical and dielectric behaviors of the matrix is performed.

2 | MATERIALS AND METHODS

2.1 | Matrix

The epoxy matrix used in this study is a mixture of MBDA (4,4′-methylenebis(N,N-diglycidylaniline)), DGEBA (diglycidyl ether of bisphenol A), and DGEBF (diglycidyl ether of bisphenol-F). The amine hardener is composed by a DETDA (diethyl toluene diamine) and a DACH (1,2 diamino cyclohexane) supplied by Sicomin/France for RTM structural applications.

2.2 | Silver nanowires

Metallic fillers are silver nanowires (AgNWs) are produced by a polyol method first developed by Sun et al.[22,23] and Wiley et al.[24] Silver nanowires were elaborated with a modified polyol process[17,18] by reducing $AgNO_3$ with ethylene glycol solution. The growth was assisted by poly(vinylpyrrolidone) which is preferentially adsorbed on {100} crystal faces of the silver seeds. The reaction occurs at 165°C under stirring in a triple-neck round-bottom flask during 40 minutes. The ratio between the reactants was adapted.[17,18] Silver nanowires were washed and stored in ethanol and the aspect ratio is around 220[18] with the following dimensions: a diameter around 200 nm and a length of 40 μm. This method allows us to obtain large quantity, up to 100 g.

2.3 | Composite processing

Composite samples were elaborated by mixing AgNWs dispersed in ethanol in the epoxy part, then the hardener was poured (stoichiometric ratio 75/25 in weight). The final suspension containing epoxy resin and silver nanowires was obtained by ultrasonic stirring.

The sample implementations were carried out in a polytetrafluoroethylene mold with two geometries: bar and disk shapes, for, respectively, mechanical and dielectric studies. After deposition, the coating was usually cured for different steps between 40°C and 200°C. The dimensions of the bar sample are 50 × 10 × 0.7 mm^3 and the disks are 200 μm thick with a diameter of 40 mm.

The AgNWs content was determined by thermogravimetric analysis (TGA) from room temperature to 1000°C at a heating rate of 20°C.min^{-1} under synthetic air atmosphere.

2.4 | Scanning electron microscopy

The quality of the dispersion was observed by electronic microscopy on a JEOL JSM 6700F instrument under a voltage between 10 and 19 keV. Backscattered electron detection mode was used to increase the contrast between AgNWs and the epoxy matrix.

2.5 | Dynamic mechanical analysis

Dynamic mechanical analyses (DMA) were carried out on an ARES G1 (Rheometrics Scientific, USA) strain controlled rheometer. Measurements were performed in the rectangular torsion mode, between −140°C to 230°C, with an angular frequency $\omega = 1$ rad.s^{-1}, and a heating rate of 3°C.min^{-1}.

2.6 | Dynamic dielectric spectroscopy

The study of electrical relaxations was carried out, thanks to a dynamic dielectric spectrometer (DDS) BDS 4000 (Novocontrol, Germany). The used frequency range was 10^{-2} to 10^6 Hz between −150°C and 200°C by 5°C steps.

The dielectric relaxation modes were fitted with the Havriliak–Negami parametric equation (Equation 1),[25,26] which defines the mean dipolar relaxation time τ_{HN}:

$$\varepsilon^*(\omega) = \varepsilon_\infty + \frac{\varepsilon_s - \varepsilon_\infty}{[1 + (i\omega\tau_{\mathrm{HN}})^{\alpha_{\mathrm{HN}}}]^{\beta_{\mathrm{HN}}}} \quad (1)$$

where ε_s and ε_∞ are, respectively, the low and high frequency limits of $\varepsilon'(\omega, T)$, τ_{HN} is the relaxation time of the electric dipole, α_{HN} and β_{HN} are the adjustable parameters, respectively, for the width and the asymmetry of the distribution, varying between 0 and 1.

The relaxation maps could be widely influenced by dissipative losses due to ohmic conduction. It implies a low resolution of the other dielectric relaxations.[27–29] In order to overcome these drawbacks, the data were adjusted by the Kramers–Kronig relations (Equation 2).[30]

$$\varepsilon''_{KK}(\omega_0) = \frac{\sigma_{DC}}{\varepsilon_0\omega_0} + \frac{2}{\pi}\int_0^\infty \varepsilon'(\omega_0)\frac{\omega_0}{\omega^2 - \omega_0^2}d\omega \quad (2)$$

where σ_{DC} is the ohmic conductivity and ε_0 is the vacuum permittivity ($8.82\,\mathrm{pF.m^{-1}}$).

The relaxation times, τ_{HN}, have been plotted on an Arrhenius diagram $\tau_{HN} = f\left(\frac{1000}{T}\right)$. The relaxation times exhibit a linear behavior corresponding to a thermal activation of the molecular mobility. In the glassy state, the temperature dependence of the relaxation times can be fitted with the Arrhenius equation (Equation 3).

$$\tau(T) = \tau_0^A e^{\frac{\Delta H}{RT}} \quad (3)$$

where $\tau_0^A = \frac{h}{k_B T}e^{-\frac{\Delta S}{R}}$ is the pre-exponential factor, h is the Planck constant, k_B is the Boltzmann constant, T is the temperature in K, ΔS is the activation entropy in $\mathrm{J.K^{-1}}$, R is the gas constant in $\mathrm{J.mol^{-1}.K^{-1}}$, and ΔH is the activation enthalpy in $\mathrm{J.mol^{-1}}$.

The linear regression analysis of experimental points allows us to determine the activation enthalpy of relaxations.

3 | RESULTS AND DISCUSSION

3.1 | Influence of chemical composition and hydration

3.1.1 | Mechanical behavior

The modification of the composition comes from the process of elaboration of a conductive coating. In order to overcome the solubility and the vaporization of part of hardener and resin with the solvents used during the spraying implementation, an excess of hardener was used. The respective mass proportions of epoxy resin and hardener were 75/25 instead of the preconized ratio (79/21). The influence of the epoxy/amine ratio on the physical structure and the cure kinetic was investigated in a previous work.[21] For this purpose, four compositions (70/30, 75/25, 79/21, and 80/20) were prepared for the mechanical study.

The DMA study was carried out on dry samples previously subjected to three temperature ramps in order to stabilize cross linking (Figure 1). The DMA thermograms exceed the maximum temperature of the curing program, that is, 200°C in order to observe the rubbery plateau.

Figure 1 highlights the mechanical behavior of epoxy samples with different ratios of hardener. The value of the storage modulus and the temperatures of the loss modulus peaks are reported in Table 1. For the storage modulus in the glassy state, the lower percentage of hardener induces an increase in its value between −140°C and 20°C. It is explained by a higher conversion degree near the equilibrium stoichiometry (79/21) with a higher rigidity of the network.[21] Above 100°C, the modulus decreases due to the mechanical manifestation of the glass transition. The rubbery plateau is also widely impacted by the variation of the stoichiometry. Upon an excess of hardener, its value is divided by two: This evolution can be explained by a fast gelation of the matrix during the curing inducing a lower cross linking density.

The loss modulus shows two major relaxation modes, β and α. The first one, β, is associated with the mobility of the OH groups of hydroxypropylethers[31–33] and diphenyl groups.[34,35] The second one, α, corresponds to the viscoelastic transition. T_β is not modified by the hardener excess while for the α relaxation, this excess induces

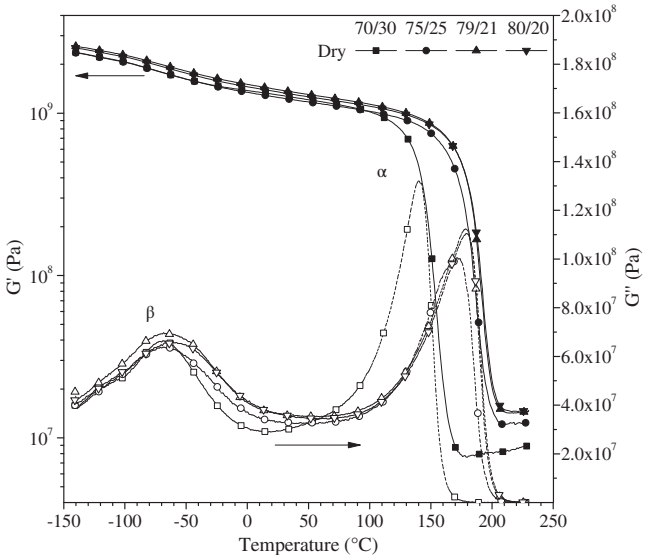

FIGURE 1 Storage modulus G' (filled symbols) and loss modulus G'' '(open symbols) as a function of temperature for four compositions of dry epoxy

	$G'_{g,-140°C}$ (Pa)	$G'_{g,20°C}$ (Pa)	$G'_{r,220°C}$ (Pa)	T_β (°C)	T_α (°C)
70/30	$2.41.10^9$ (0.06)	$1.34.10^9$ (0.04)	$0.88.10^7$ (0.04)	−68 (1)	139 (2)
75/25	$2.2.10^9$ (0.1)	$1.21.10^9$ (0.06)	$1.22.10^7$ (0.04)	−67 (2)	171 (0)
79/21	$2.57.10^9$ (0.01)	$1.41.10^9$ (0.01)	$1.45.10^7$ (0.02)	−67 (1)	179 (1)
80/20	$2.51.10^9$ (0.01)	$1.37.10^9$ (0.01)	$1.44.10^7$ (0.02)	−63 (2)	180 (0)

TABLE 1 Storage modulus G' in the glassy state (G'_g) and in the rubbery state (G'_r); temperatures of the α and β relaxation modes of loss modulus G' for different compositions (uncertainties are added)

for T_α a decrease of 40°C. This variation is also due to the lower amount of cross linking that make the molecular mobility easier. The presence of unreacted hardener molecules might play the role of plasticizer.

The moisture involves different effects on the polymer matrix such as dimensional variations[36,37] or modifications of the mechanical properties.[38,39] The phenomenological mechanisms of the water diffusion are described by the first Fick's Law.[40,41] Here, only the consequence on the physical properties will be reported. The water absorption is due to the diffusion into the 3D network and the polar attraction of the hydroxyl groups.[42] In order to evaluate the influence of moisture on the epoxy matrix, samples with different ratios (70/30, 75/25, 79/21, and 80/20) with a disk shape (diameter: 52 mm; thickness: 1, 3 mm) were immerged into deionized water. For each stoichiometry, four samples were prepared. Figure 2 shows that the moisture uptake tends to a plateau close to 60 days at about 3.25 wt% of water. These values are consistent with the ones reported in the literature.[39,43] After 392 days, the samples with an excess of hardener shows a higher moisture uptake. The values for the chemical compositions 70/30, 75/25, 79/21, and 80/20 are respectively: $4.22 \pm 0.06\%$, $3.86 \pm 0.01\%$, $3.81 \pm 0.06\%$, and $3.41 \pm 0.09\%$. This result could be associated to a more important free volume into the matrix with an excess of hardener due to a lower relative degree of conversion.[21] The presence of free molecules of hardener, DACH and DETDA, may induce a higher water sorption because of their polarity.

The DMA analyses on wet samples were performed on the dry 75/25 epoxy which is used as matrix for conductive coatings.

Figure 3 and Table 2 show the moisture influence on the mechanical properties of the epoxy. For the storage modulus in the glassy state, moisture induces an increase in the value at −140°C and 20°C. It can be explained by physical interactions between H_2O molecules and hydroxyl groups. For the temperatures below 0°C, frozen water rigidifies the structure which implies this increase; above 0°C physical interactions limit molecular mobility.

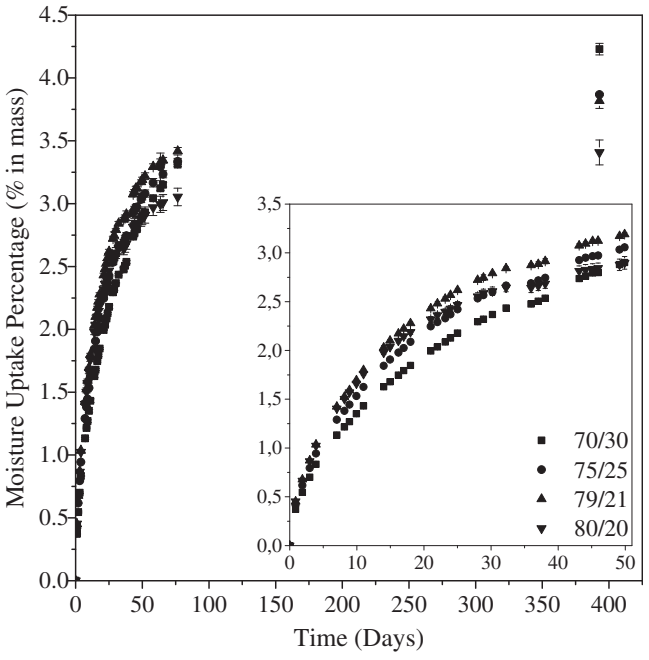

FIGURE 2 Epoxy moisture uptake as a function of time t, for the various compositions. The framed details represent the variation for the first days

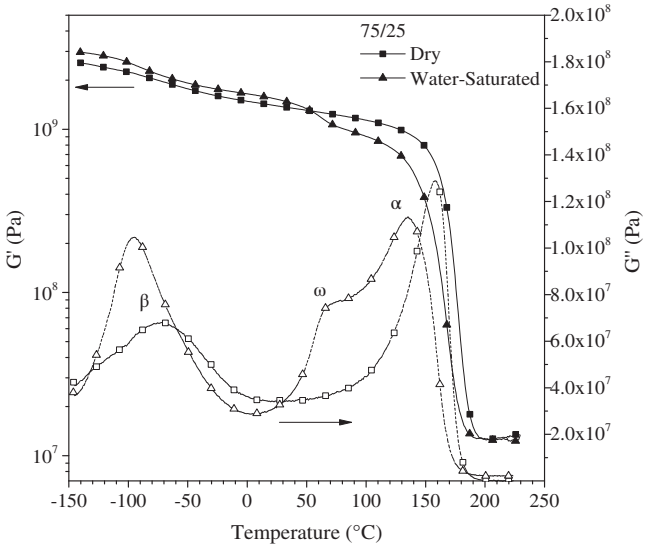

FIGURE 3 Storage modulus G' and loss modulus G'' as a function of temperature for dry and wet 75/25 epoxy

TABLE 2 Storage modulus G' in the glassy state (G'_g) and in the rubbery state (G'_r); temperatures of the β, ω, and α relaxation modes for dry and wet 75/25 epoxy

	$G'_{g,\ -140°C}$ (Pa)	$G'_{g,\ 20°C}$ (Pa)	$G'_{r,220°C}$ (Pa)	T_β (°C)	T_ω (°C)	T_α (°C)
Dry	$2.6.10^9$	$1.4.10^9$	$1.3.10^7$	−66	N/A	164
Wet	3.10^9	$1.6.10^9$	$1.2.10^7$	−89	84	141

The rubbery plateau remains unmodified. The loss modulus shows three major relaxation modes: β, ω, and α in the order of increasing temperature. In comparison with the dry sample, the β relaxation mode is widely amplified upon water and it is shifted to lower temperatures. The origin of this relaxation could explain this phenomenon: OH groups of hydroxypropylethers are impacted by the presence of water due to their polar nature.[31–33] Around 80°C, a new relaxation, ω is observed. It is associated with the relaxation of the heterogeneities such as unreacted products or dangling chains that are missing in the dry state.[43–46]

The temperature of the anelastic manifestation of the glass transition, α, decreases by 20°C in wet condition due to the plasticization phenomenon.

3.1.2 | Dielectric behavior

The influence of the chemical composition (70/30, 75/25, and 80/20) on molecular mobility of epoxy in dry condition was investigated by DDS. Figure 4 shows the dielectric loss ε''_{KK} as a function of temperature and frequency after a Kramers–Kronig (KK) treatment. The β and α dielectric relaxation modes are similar to the ones obtained with DMA (cf. Figure 1). The flow, σ, at high temperature and low frequency is always present despite the KK treatment. It indicates ions accumulation at electrode-sample interfaces.[27] The value of $\Delta\varepsilon''_{KK}$ for the α relaxation is higher (Table 3) than the one generally obtained for polymer matrices (around 10^{-1}).[47–49]

Figure 5 shows the relaxation time as a function of temperature on an Arrhenius diagram for epoxy with the various epoxy/amine ratio in the dry state. The value of ΔH (Table 3) depends on the chemical composition: The hardener excess induces a decrease of ΔH. Previous work showed that, upon excess of hardener, the degree of conversion is lower, and crosslinking decreases.[21] These findings are consistent with our DMA data (Table 1 and Figure 1). The activation enthalpy of the α relaxation decreases, but we observe an increase in its value when the excess increase again (70/30). It might be attributed to physical interactions with the large quantity of

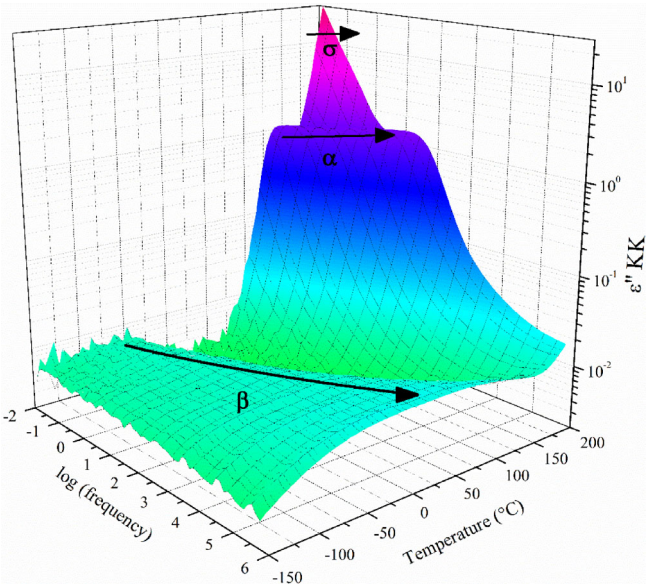

FIGURE 4 Dielectric loss ε''_{KK} versus temperature and frequency for 80/20 epoxy in dry condition [Color figure can be viewed at wileyonlinelibrary.com]

unreacted molecules that induces a decrease in the steric mobility. The activation enthalpy of the β mode is not clearly modified by the variation of the epoxy/amine ratio due to the localized character of this relaxation mode.

Table 4 lists the values of the parameters extracted from the Arrhenius diagram. The linear regression of the data points for the α mode exhibits a discontinuity close to T_α and $T_{g,\text{calorimetry}}$.[21] This modification and the high value of $\Delta\varepsilon''_\alpha$ indicate that the α relaxation is not only due to the increase in molecular mobility near the glass transition. The increase of ΔH after T_α and T_g (Figure 5b and Table 4) implies the transition from an electronic contribution to an ionic one. The enthalpy recorded at higher temperature is consistent with the literature for a protonic contribution.[48] This ionic contribution could come from the mobility of unreacted molecules liberated near the glass transition. This hypothesis is supported by the high value of $\Delta\varepsilon''_\alpha$ (Table 3).

The water aging was investigated with the same methodology than for the mechanical study: The analysis was focused on the sample with the epoxy/amine ratio 75/25. The dielectric loss ε''_{KK} surface is presented in Figure 6. It exhibits five major relaxation modes. At low temperature, a γ mode is observed on the low temperature side of the β relaxation. The ω mode is observed like on DMA G″ thermograms. It might have the same origin (Figure 3).

The Arrhenius diagram of the resolved modes for the dry and hydrated 75/25 epoxy is reported in Figure 6b. The activation parameters are indicated in Table 5. They

TABLE 3 Arrhenius parameters for the α and β modes for epoxy with different epoxy/amine ratio

	70/30		75/25		80/20	
Contribution	τ_0 **(s)**	ΔH **(kJ.mol^{-1})**	τ_0 **(s)**	ΔH **(kJ.mol^{-1})**	τ_0 **(s)**	ΔH **(kJ.mol^{-1})**
α	$8.3.10^{-24}$	187 ± 4	$7.6.10^{-21}$	169 ± 4	$1.2.10^{-28}$	234 ± 10
β	$2.7.10^{-17}$	66 ± 2	$1.1.10^{-16}$	64 ± 1	$6.8.10^{-18}$	70.1 ± 0.5
$\Delta\varepsilon''_\alpha$	8		17		1	

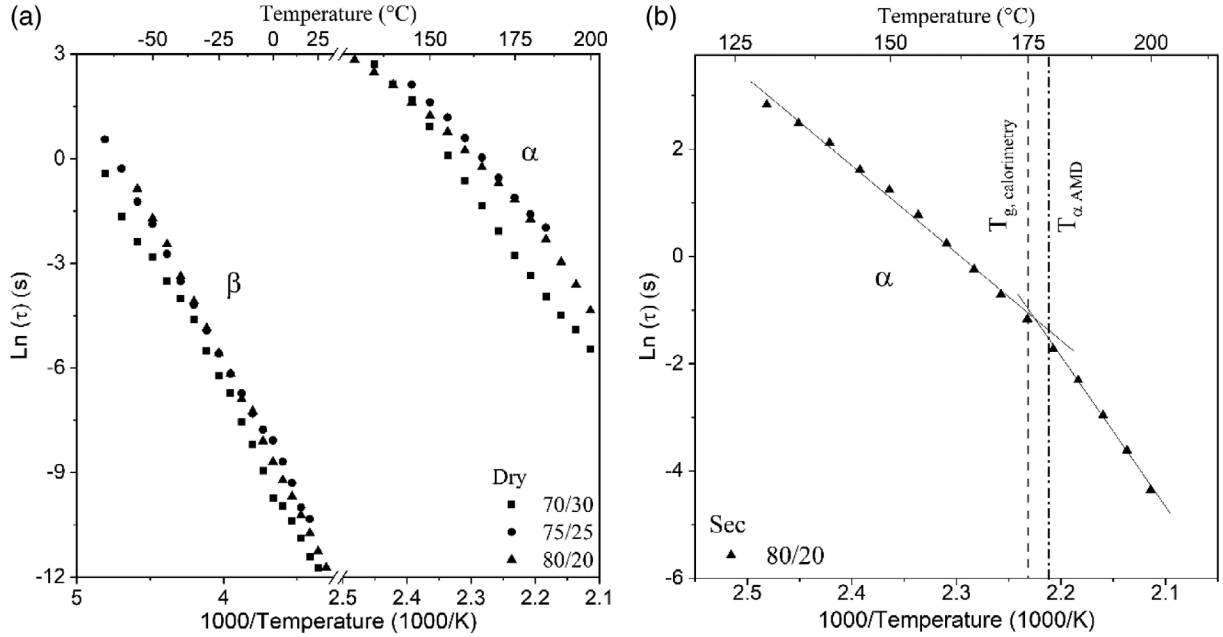

FIGURE 5 (a) Arrhenius diagram of dielectric relaxations times of epoxy for different epoxy/amine ratios in dry condition. (b) Arrhenius diagram of α relaxation times of 80/20 epoxy in dry condition

TABLE 4 Arrhenius parameters for the α relaxation before and after $T_{g\,\text{calorimetry}}$

		70/30		80/20	
Contribution	**Temperature**	τ_0 **(s)**	ΔH **(kJ.mol^{-1})**	τ_0 **(s)**	ΔH **(kJ.mol^{-1})**
α	$< T_{g\,\text{calorimetry}}$	$2.6.10^{-18}$	147 ± 10	$1.1.10^{-16}$	135 ± 5
α	$> T_{g\,\text{calorimetry}}$	$8.3.10^{-24}$	187 ± 4	$1.2.10^{-28}$	234 ± 10

highlight the influence of moisture on the activation enthalpies of the relaxation modes. The lowest value is recorded for the γ mode that corresponds to a localized mobility of small relaxing units. The β relaxation mode is sensitive to hydration: a decrease of 20% of the activation enthalpy is observed upon hydration. This behavior was widely reported in the literature[50,51] as a plasticization phenomenon. This shift toward lower temperature allows the resolution of the γ mode upon hydration. The ω relaxation could not be adjusted with the Havriliak–Negami equation (Equation 1) since its maximum is not defined over a significant frequency range. Just like for the β mode, the activation enthalpies of the α mode decreases by 7% upon hydration: the plasticization phenomenon makes easier the molecular mobility.

3.2 | Influence of silver nanowires

3.2.1 | Dispersion in the matrix

Silver nanowires dispersion in the epoxy coating matrix was observed with a scanning electron microscope (SEM). This observation (Figure 7) shows a homogenous

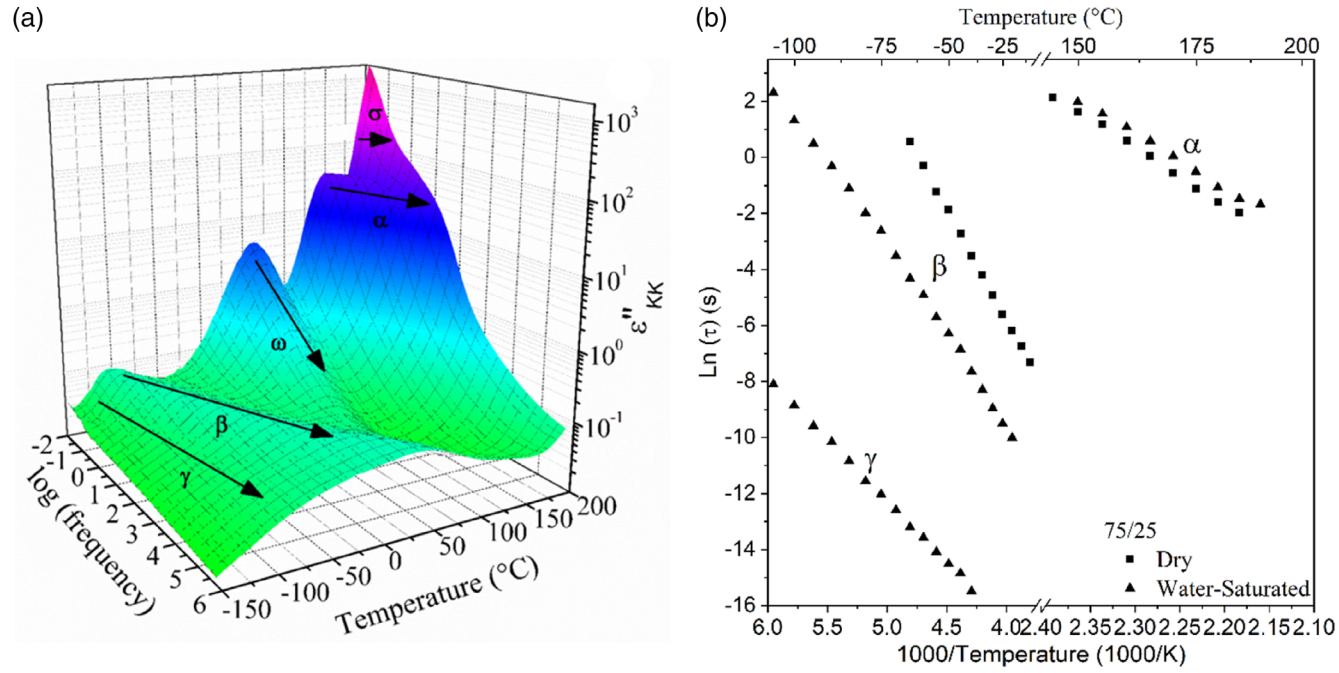

FIGURE 6 (a) Dielectric loss ε''_{KK} surface for the hydrated 75/25 epoxy. (b) Arrhenius diagram of dielectric relaxations times of epoxy 75/25 in dry and hydrated conditions [Color figure can be viewed at wileyonlinelibrary.com]

TABLE 5 Arrhenius parameters of dielectric relaxations of 75/25 epoxy in dry and hydrated conditions

	Dry		Wet	
Contribution	τ_0 **(s)**	ΔH **(kJ.mol^{-1})**	τ_0 **(s)**	ΔH **(kJ.mol^{-1})**
α	$7.6.10^{-21}$	169 ± 4	$4.3.10^{-19}$	158 ± 6
β	$1.1.10^{-16}$	64 ± 1	$1.4.10^{-15}$	51 ± 1
γ	N/A	N/A	$1.4.10^{-15}$	36.4 ± 0.4

dispersion of the AgNWs. The high aspect ratio of AgNWs was preserved after the process.

3.2.2 | Electrical behavior

Epoxy/AgNWs composite behavior

The study of the AgNWs influence on dielectric relaxations can be investigated only for filler contents below the electrical percolation threshold, that is, 0.7 vol% with this system.[21] In this work, the AgNWs content is 0.3 vol % and the study was performed on dry samples. The dielectric loss ε''_{KK} surface in Figure 8 shows the two major relaxation modes, β and α. The Kramers Kronig treatment does not permit to extract the ω relaxation due to the high influence of the α and σ modes. The value of $\Delta\varepsilon''_{KK}$ for the α relaxation is higher than for the other configurations. This observation shows that the α relaxation is not only due to the increase in molecular mobility. Indeed, its magnitude is three decades higher than that for other polymer matrixes.[47–49] This behavior could be explained by an increase in free electronic charges that produces an increase in the dissipative component of the permittivity induced by the AgNWs.

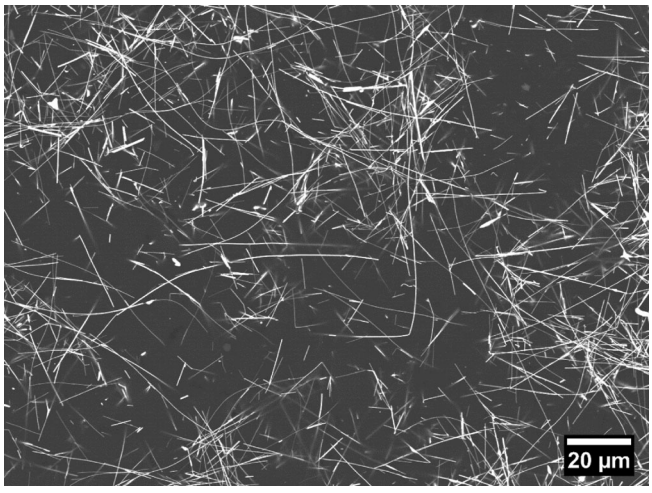

FIGURE 7 SEM images of epoxy/Ag 1 vol% AgNWs

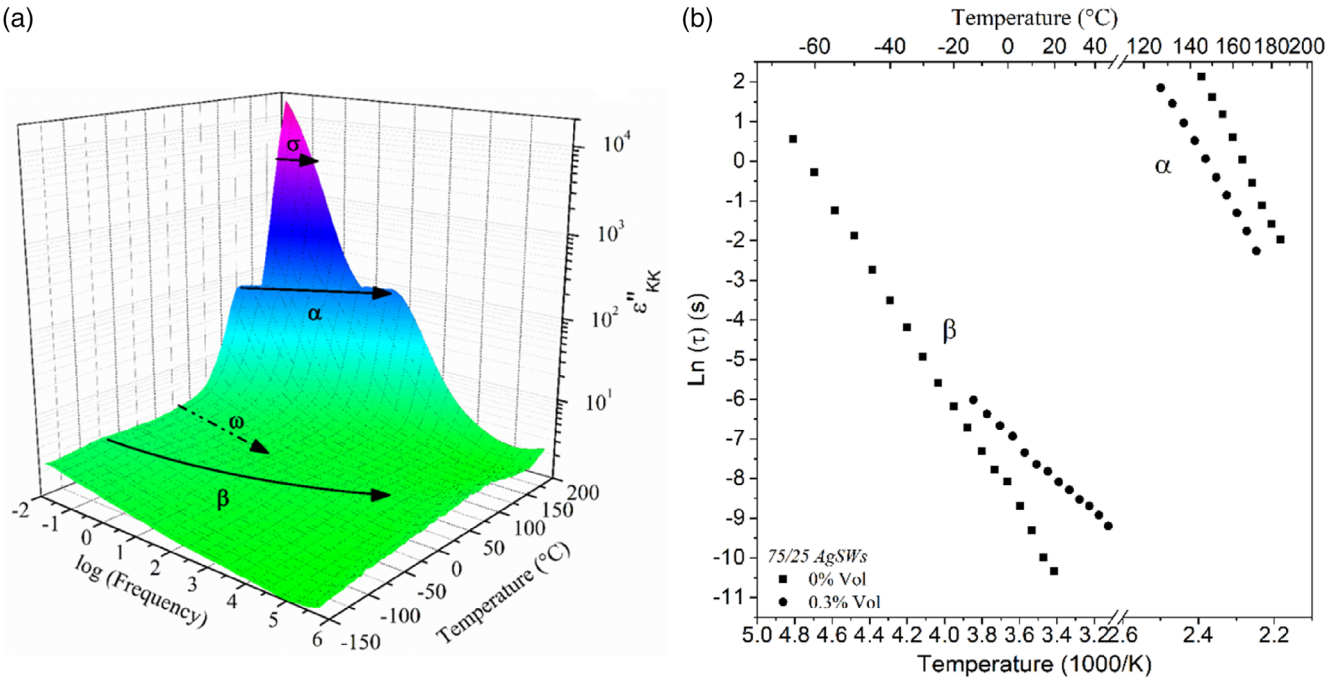

FIGURE 8 (a) Dielectric loss ε''_{KK} surface of a 75/25 epoxy/0.3 vol% AgNWs composite in dry condition. (b) Arrhenius diagram of dielectric relaxations times of a 75/25 epoxy/AgNWs 0.3 vol% composite in dry condition [Color figure can be viewed at wileyonlinelibrary.com]

	0 vol% AgNWs		0.3 vol% AgNWs	
Contribution	τ_0 (s)	ΔH (kJ.mol^{-1})	τ_0 (s)	ΔH (kJ.mol^{-1})
α	$7.6.10^{-21}$	169 ± 4	$1.5.10^{-17}$	135 ± 3
β	$1.1.10^{-16}$	64 ± 1	$1.4.10^{-10}$	36 ± 1

TABLE 6 Arrhenius parameters of dielectric relaxations of the 75/25 epoxy and the epoxy/AgNWs 0.3 vol% composite in dry condition

In Figure 8b, a linear behavior of relaxation times as a function of reciprocal temperature is observed for composites: There is no change of slope near the $T_{g,calorimetry}$. This behavior could be explained by a preponderance of the electronic contribution upon the ionic one due to the high amount of electrons provided by the AgNWs.

The introduction of nanofillers induces a decrease in the activation enthalpy for both relaxation modes (Table 6). The first explanation is a lower conversion degree due to AgNWs which create steric hindrance, increase in viscosity, and decrease in molecular mobility during crosslinking. The crosslink density is lower which implies a higher degree of freedom. In addition, the thermal conductivity increases, thanks to the metallic fillers[7]; this evolution favors molecular mobility.

Electrical performance

The AgNWs are introduced for increasing the electrical conductivity of the epoxy composite coating for the LSP of the aircraft. The electrical conductivity level increases with the amount of the AgNWs to reach 4.10^2 S.m^{-1} at 8 vol% for the sample geometry used for DDS experiments.[21] This configuration does not really fulfill the requirements of Pouillet's law (Equation 4)[52–54] because the length (here the thickness) of the samples is lower than the diameter.

$$R = \rho\frac{l}{S} = \sigma\frac{S}{l} \tag{4}$$

where R is the electrical resistance measured in Ohm, ρ is the resistivity of the sample in Ω.m, l is the length of the channel in m, S is the section of the channel m^2, and σ is the electrical conductivity in S.m^{-1}.

A previous study was carried out with a correct geometry of the samples and permitted to obtain higher value of the conductivity: $5.5.10^5$S.m^1 at 60°C for 9 vol% of AgNWs.[55] This value is one of the highest reported in the literature for this kind of composite with such a low filler ratio.

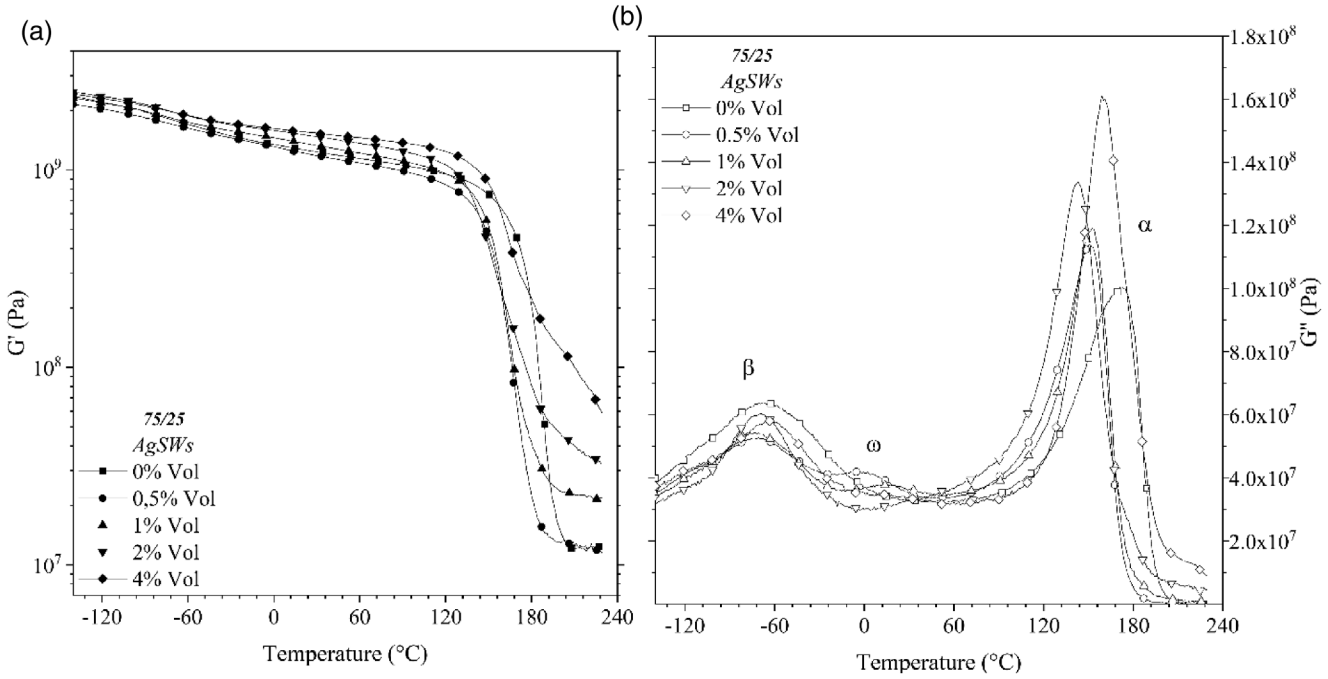

FIGURE 9 (a) Storage modulus G' as a function of temperature for dry 75/25 epoxy/AgNWs composites. (b) Loss modulus G'' as a function of temperature for dry 75/25 epoxy/AgNWs

TABLE 7 Storage modulus G' in the glassy state (G'_g) and in the rubbery state (G'_r) for different AgNWs contents (uncertainties are added)

	$G'_{g,-140°C}$ (Pa)	$G'_{g,20°C}$ (Pa)	$G'_{r,220°C}$ (Pa)
0 vol%	$2.2.10^9$ (0.1)	$1.21.10^9$ (0.06)	$1.22.10^7$ (0.04)
0.5 vol%	$2.2.10^9$ (0.8)	$1.25.10^9$ (0.04)	$1.1.10^7$ (0.2)
1 vol%	$2.5.10^9$ (0.2)	$1.5.10^9$ (0.1)	$1.9.10^7$ (0.5)
2 vol%	$2.8.10^9$ (0.4)	$1.8.10^9$ (0.4)	$3.7.10^7$ (0.1)
4 vol%	$2.5.10^9$ (0.1)	$1.61.10^9$ (0.01)	5.10^7 (2)

TABLE 8 Temperatures of the relaxation modes as a function of the AgNWs content

	T_β (°C)	T_ω (°C)	T_α (°C)
0 vol%	−68	N/A	171
0.5 vol%	−70	−5	150
1 vol%	−74	13	152
2 vol%	−69	33	144
4 vol%	−64	N/A	159

3.2.3 | Mechanical behavior

The DMA study was performed on composites with: 0.5 vol%, 1 vol%, 2 vol%, and 4 vol% as filler content; the epoxy/amine ratio was 75/25 for all the samples. Each thermogram was obtained after three scans in order to avoid any evolution of the physical structure during measurements.

Storage modulus

Figure 9 and Table 7 highlight the influence of AgNWs on the storage modulus. The influence on the glassy plateau at −140°C is weak due to the rigidity of the neat matrix. At 20°C, an increase about 30% is observed for the 2 vol% composite. This phenomenon was already observed in similar configurations.[15,18] The fillers reinforce the matrix and induce an increase in the storage modulus. This phenomenon is more important on the rubbery plateau that is multiplied by 5 for the epoxy filled with 4 vol% of AgNWs composite. AgNWs acts as topological nodes that highly modify the rubbery flow.

Loss modulus

Figure 9b and Table 8 show the influence of the AgNWs on the anelastic relaxation modes. The temperature T_β varies as a function of filler content. The initial decrease is followed by an increase of T_β. The first phenomenon might be due to the increase in the thermal conductivity.[7] The second one has been associated with the steric hindrance exerted by AgNWs on polymeric sequences.[21] The relaxation mode ω is observable for the dry state of the composite. Taking as reference the ω mode observed in the hydrated state of the matrix (Figure 3), the relaxation

temperature for the composite is shifted toward lower temperature. Furthermore, we have observed a decrease in its amplitude after several heatings. The highest amplitude is obtained with the highest filler content. This mode is an indicator of the heterogeneities in the matrix. The AgNWs induce steric hindrance which limits the relative degree of conversion[21] and increase the amount of unreacted products inside the matrix. The lower value of T_ω indicates the weak size of heterogeneities. The temperature of the anelastic manifestation of the glass transition, α, decrease of 20°C. For the lowest filler content, it might be due to a better thermal conductivity; for the highest, it has been associated to a lower crosslinks density. The area of the α relaxation is higher with AgNWs; this is characteristic of a stick–slip phenomenon. A similar increase in energy loss at the α relaxation has been reported for a wide variety of composites.[18,56–59]

4 | CONCLUSION

DMA and DDS were used to study the dynamic molecular mobility of an epoxy matrix in dry and wet states and its composites epoxy/silver nanowires. The combination of both methods allows us to make correlations to identify the molecular origin of those mechanisms.

The influence of the epoxy/amine ratio on the mechanical properties was observed: The excess of hardener implies an increase in the unreacted chains and a decrease in cross links density. Accordingly, the storage modulus on the rubbery plateau decreases. The loss modulus highlights for dry samples two major relaxations, β and α. The temperature of the anelastic manifestation of the glass transition, $T\alpha$, decreases upon the hardener excess due to the same reasons. Dielectric spectroscopy shows an interesting modification of the activation enthalpy close to the calorimetric glass temperature. It has been associated to the transition between an electronic diffusion to an ionic one, thanks to the increase in free volume. This hypothesis is supported by the high value of $\Delta\varepsilon''_{KK}$.

For hydrated samples, mechanical relaxation modes are modified: For the β mode, there is a shift toward lower temperatures and an increase in the magnitude. The dielectric spectroscopy shows a reduction of the activation enthalpy of these modes in hydrated conditions due to a plasticization phenomenon. The analysis of the α relaxation in hydrated conditions shows the existence of two supplementary relaxation modes. The first one, γ, at lower temperature is due to a localized molecular mobility. The second one, ω, is noticeable on both mechanical and dielectric relaxation spectra. It is due to the heterogeneities of the 3D network more severe in hydrated conditions.

The introduction of AgNWs has practically no effect on the mechanical properties of the glassy state. For the rubbery state, AgNWs cause an increase in the storage modulus as a function of the filler content. The loss modulus profile is modified: the ω relaxation is present in dry condition at a lower temperature. The magnitude of the α mode is increased due to the stick–slip phenomenon. Moreover, it is shifted toward lower temperatures. In other words, the activation enthalpy decreases for both modes. Electrical study through DDS and conductivity measurement of composites shows the consequence of a lower relative degree of conversion caused by the insertion of AgNWs. The transition between an electronic diffusion to an ionic one is no longer visible and the value of $\Delta\varepsilon''_{KK}$ is higher. This behavior is a characteristic of the large amount of electrons due to nanowires.

The introduction of AgNWs allows us to obtain one of the highest values of the electrical conductivity for polymer-based composites without any drastic evolution of mechanical properties.

ACKNOWLEDGMENTS

These results were obtained under the research project "COMPINNOVTD" at the IRT Saint Exupéry. We thank the industrial and academic members of the IRT who supported this project through their contributions, both financial and in terms of specific knowledge:

- Industrial members: Airbus Operations, ArianeGroup, Airbus Helicopters, Airbus Group Innovations, STELIA Aerospace and Thales Alenia Space.
- Academic members: CIRIMAT, UPS and CNRS.

We also thank the Commissariat Général aux Investissements and the Agence Nationale de la Recherche for their financial support in the Programme d'Investissement d'Avenir (PIA).

ORCID

Antoine Lonjon https://orcid.org/0000-0002-4346-6543

REFERENCES

[1] M. Holmes, *Reinf. Plast.* **2014**, *58*, 38. https://doi.org/10.1016/S0034-3617(14)70251-6

[2] A. Lonjon, P. Demont, E. Dantras, C. Lacabanne, *J. Non-Cryst. Solids* **2012**, *358*, 1859. https://doi.org/10.1016/j.jnoncrysol.2012.05.038

[3] M. Gagné, D. Therriault, *Prog. Aerosp. Sci.* **2014**, *64*, 1. https://doi.org/10.1016/j.paerosci.2013.07.002

[4] F. A. Fisher, J. A. Plumer, Lightning Protection of Aircraft, **1977**. http://ntrs.nasa.gov/archive/nasa/casi.ntrs.nasa.gov/19780003081.pdf.

[5] C. Karch, C. Paul, F. Heidler, in *2019 Int. Symp. Electromagn. Compat. - EMC Eur.*, *Lightning Strike Protection of Radomes*,

IEEE, 2019, 650–655. https://doi.org/10.1109/EMCEurope.2019.8871944.
[6] M. Ali Raza, A. Westwood, C. Stirling, R. Brydson, N. Hondow, *J. Appl. Polym. Sci.* **2012**, *126*, 641. https://doi.org/10.1002/app.36655
[7] L. Rivière, A. Lonjon, E. Dantras, C. Lacabanne, P. Olivier, N. R. Gleizes, *Eur. Polym. J.* **2016**, *85*, 115. https://doi.org/10.1016/j.eurpolymj.2016.08.003
[8] D. Untereker, S. Lyu, J. Schley, G. Martinez, L. Lohstreter, *ACS Appl. Mater. Interfaces* **2009**, *1*, 97. https://doi.org/10.1021/am800038z
[9] A. Lonjon, L. Laffont, P. Demont, E. Dantras, C. Lacabanne, *J. Phys. Chem. C* **2009**, *113*, 12002. https://doi.org/10.1021/jp901563w
[10] J. Audoit, L. Laffont, A. Lonjon, E. Dantras, C. Lacabanne, *Polymer (Guildf)* **2015**, *78*, 104. https://doi.org/10.1016/j.polymer.2015.09.062
[11] T. H. L. Nguyen, L. Quiroga Cortes, A. Lonjon, E. Dantras, C. Lacabanne, *J. Non-Cryst. Solids* **2014**, *385*, 34. https://doi.org/10.1016/j.jnoncrysol.2013.11.008
[12] S. Wang, Y. Cheng, R. Wang, J. Sun, L. Gao, *ACS Appl. Mater. Interfaces* **2014**, *6*, 6481. https://doi.org/10.1021/am500009p
[13] L. Ramachandran, A. Lonjon, P. Demont, E. Dantras, C. Lacabanne, *Mater. Res. Express.* **2016**, *3*, 085027. https://doi.org/10.1088/2053-1591/3/8/085027
[14] J. Stejskal, *Chem. Pap.* **2013**, *67*, 814. https://doi.org/10.2478/s11696-012-0304-6
[15] A. Lonjon, P. Demont, E. Dantras, C. Lacabanne, *J. Non-Cryst. Solids* **2012**, *358*, 236. https://doi.org/10.1016/j.jnoncrysol.2011.09.019
[16] I. Moreno, N. Navascues, S. Irusta, J. Santamaría, *IOP Conf. Ser. Mater. Sci. Eng.* **2012**, *40*, 012001. https://doi.org/10.1088/1757-899X/40/1/012001
[17] A. Lonjon, I. Caffrey, D. Carponcin, E. Dantras, C. Lacabanne, *J. Non-Cryst. Solids* **2013**, *376*, 199. https://doi.org/10.1016/j.jnoncrysol.2013.05.020
[18] L. Q. Cortes, A. Lonjon, E. Dantras, C. Lacabanne, *J. Non-Cryst. Solids* **2014**, *391*, 106. https://doi.org/10.1016/j.jnoncrysol.2014.03.016
[19] S. Kirkpatrick, *Rev. Mod. Phys.* **1973**, *45*, 574. https://doi.org/10.1103/RevModPhys.45.574
[20] I. Balberg, C. H. Anderson, S. Alexander, N. Wagner, *Phys. Rev. B* **1984**, *30*, 3933. https://doi.org/10.1103/PhysRevB.30.3933
[21] V. Bedel, A. Lonjon, É. Dantras, M. Bouquet, *J. Appl. Polym. Sci.* **2018**, *135*, 46829. https://doi.org/10.1002/app.46829
[22] Y. Sun, Y. Yin, B. T. Mayers, T. Herricks, Y. Xia, *Chem. Mater.* **2002**, *14*, 4736. https://doi.org/10.1021/cm020587b
[23] Y. Sun, Y. Xia, *Adv. Mater.* **2002**, *14*, 833. https://doi.org/10.1002/1521-4095(20020605)14:11<833::AID-ADMA833>3.0.CO;2-K
[24] B. Wiley, Y. Sun, Y. Xia, *Acc. Chem. Res.* **2007**, *40*, 1067. https://doi.org/10.1021/ar7000974
[25] S. Havriliak, S. Negami, *J. Polym. Sci. Part C Polym. Symp.* **2007**, *14*, 99. https://doi.org/10.1002/polc.5070140111
[26] S. Havriliak, S. Negami, *Polymer (Guildf)* **1967**, *8*, 161. https://doi.org/10.1016/0032-3861(67)90021-3
[27] D. L. Sidebottom, B. Roling, K. Funke, *Phys. Rev. B* **2000**, *63*, 024301. https://doi.org/10.1103/PhysRevB.63.024301
[28] S. Saito, H. Sasabe, T. Nakajima, K. Yada, *J. Polym. Sci. Part A-2 Polym. Phys.* **1968**, *6*, 1297. https://doi.org/10.1002/pol.1968.160060708
[29] H. W. Starkweather, P. Avakian, *J. Polym. Sci. Part B Polym. Phys.* **1992**, *30*, 637. https://doi.org/10.1002/polb.1992.090300614
[30] P. A. M. Steeman, J. van Turnhout, *Colloid Polym. Sci.* **1997**, *275*, 106. https://doi.org/10.1007/s003960050059
[31] A. C. Grillet, J. Galy, J.-F. Gérard, J.-P. Pascault, *Polymer (Guildf)* **1991**, *32*, 1885. https://doi.org/10.1016/0032-3861(91)90380-2
[32] L. Heux, J. L. Halary, F. Lauprêtre, L. Monnerie, *Polymer (Guildf)* **1997**, *38*, 1767. https://doi.org/10.1016/S0032-3861(96)00694-5
[33] M. Ochi, M. Okazaki, M. Shimbo, *J. Polym. Sci. Polym. Phys. Ed.* **1982**, *20*, 689. https://doi.org/10.1002/pol.1982.180200411
[34] E. F. Cuddihy, J. Moacanin, *Adv. Chemother.* **1970**, *8*, 96. https://doi.org/10.1021/ba-1970-0092.ch009
[35] E. F. Cuddihy, J. Moacanin, *J. Polym. Sci. Part A-2 Polym. Phys.* **1970**, *8*, 1627. https://doi.org/10.1002/pol.1970.160080915
[36] M. J. Adamson, *J. Mater. Sci.* **1980**, *15*, 1736. https://doi.org/10.1007/BF00550593
[37] G. Z. Xiao, M. E. R. Shanahan, *Polymer (Guildf)* **1998**, *39*, 3253. https://doi.org/10.1016/S0032-3861(97)10060-X
[38] M. R. Bowditch, *Int. J. Adhes. Adhes.* **1996**, *16*, 73. https://doi.org/10.1016/0143-7496(96)00001-2
[39] Y. C. Lin, X. Chen, *Polymer (Guildf)* **2005**, *46*, 11994. https://doi.org/10.1016/j.polymer.2005.10.002
[40] V. Bellenger, J. Verdu, E. Morel, *J. Mater. Sci.* **1989**, *24*, 63. https://doi.org/10.1007/BF00660933
[41] J. Crank, *The Mathematics of Diffusion*, Clarendon Press, London **1975**.
[42] Y. Diamant, G. Marom, L. J. Broutman, *J. Appl. Polym. Sci.* **1981**, *26*, 3015. https://doi.org/10.1002/app.1981.070260917
[43] W. J. Mikols, J. C. Seferis, A. Apicella, L. Nicolais, *Polym. Compos.* **1982**, *3*, 118. https://doi.org/10.1002/pc.750030304
[44] J. D. Keenan, J. C. Seferis, J. T. Quinlivan, *J. Appl. Polym. Sci.* **1979**, *24*, 2375. https://doi.org/10.1002/app.1979.070241206
[45] I. Harismendy, R. Miner, A. Valea, R. Llano-Ponte, F. Mujika, I. Mondragon, *Polymer (Guildf)* **1997**, *38*, 5573. https://doi.org/10.1016/S0032-3861(97)00121-3
[46] G. Sanz, J. Garmendia, M. A. Andres, I. Mondragon, *J. Appl. Polym. Sci.* **1995**, *55*, 75. https://doi.org/10.1002/app.1995.070550108
[47] A. Roggero, E. Dantras, T. Paulmier, C. Tonon, N. Balcon, V. Rejsek-Riba, S. Dagras, D. Payan, *J. Phys. D. Appl. Phys.* **2015**, *48*, 135302. https://doi.org/10.1088/0022-3727/48/13/135302
[48] D. Dupenne, A. Roggero, E. Dantras, A. Lonjon, T. Pierré, C. Lacabanne, *J. Non-Cryst. Solids* **2017**, *468*, 46. https://doi.org/10.1016/j.jnoncrysol.2017.04.022
[49] H. Deligöz, S. Özgümüş, T. Yalçınyuva, S. Yıldırım, D. Değer, K. Ulutaş, *Polymer (Guildf)* **2005**, *46*, 3720. https://doi.org/10.1016/j.polymer.2005.02.097
[50] J. Mijović, H. Zhang, *Macromolecules* **2003**, *36*, 1279. https://doi.org/10.1021/ma021568q
[51] J. D. Reid, W. H. Lawrence, R. P. Buck, *J. Appl. Polym. Sci.* **1986**, *31*, 1771. https://doi.org/10.1002/app.1986.070310622
[52] J. A. Stratton, *Electromagnetic Theory*, John Wiley & Sons, Inc., Hoboken, NJ, USA **2015**. https://doi.org/10.1002/9781119134640
[53] L. J. Swartzendruber, *Correction factor tables for four-point probe resistivity measurements on thin, circular semiconductor*

samples, U.S. Department of Commerce, National Bureau of Standards, Washington, D.C. **1964** https://archive.org/details/correctionfactor199swar

[54] F. M. Smits, *Bell Syst. Tech. J.* **1958**, *37*, 711. https://doi.org/10.1002/j.1538-7305.1958.tb03883.x

[55] V. Bedel, É. Dantras, A. Lonjon, M. Bouquet, *Compos. Part A Appl. Sci. Manuf. Submitted* **2018**, *137*, 48700.

[56] C. Bessaguet, E. Dantras, C. Lacabanne, M. Chevalier, G. Michon, *J. Non-Cryst. Solids* **2017**, *459*, 83. https://doi.org/10.1016/j.jnoncrysol.2016.12.030

[57] J.-F. Capsal, C. Pousserot, E. Dantras, J. Dandurand, C. Lacabanne, *Polymer (Guildf)* **2010**, *51*, 5207. https://doi.org/10.1016/j.polymer.2010.09.011

[58] X. Zhou, E. Shin, K. W. Wang, C. E. Bakis, *Compos. Sci. Technol.* **2004**, *64*, 2425. https://doi.org/10.1016/j.compscitech.2004.06.001

[59] I. Finegan, *Compos. Sci. Technol.* **2003**, *63*, 1629. https://doi.org/10.1016/S0266-3538(03)00054-X

How to cite this article: V. Bedel, A. Lonjon, É. Dantras, M. Bouquet, C. Lacabanne, *J. Appl. Polym. Sci.* **2021**, e51710. https://doi.org/10.1002/app.51710